IMpACT: Inverse Model Accuracy and Control Performance Toolbox for Buildings

Madhur Behl, Truong X. Nghiem and Rahul Mangharam
Dept. of Electrical and Systems Engineering
University of Pennsylvania
{mbehl, nghiem, rahulm}@seas.upenn.edu

***Abstract*— Uncertainty affects all aspects of building performance: from the identification of models, through the implementation of model-based control, to the operation of the deployed systems. Learning models of buildings from sensor data has a fundamental property that the model can only be as accurate and reliable as the data on which it was trained. For small and medium size buildings, a low-cost method for model capture is necessary to take advantage of optimal model-based supervisory control schemes.**

We present IMpACT, a methodology and a toolbox for analysis of uncertainty propagation for building inverse modeling and controls. Given a plant model and real input data, IMpACT automatically evaluates the effect of the uncertainty propagation from sensor data to model accuracy and control performance. We also present a statistical method to quantify the bias in the sensor measurement and to determine near optimal sensor placement and density for accurate signal measurements. In our previous work, we considered the end-to-end propagation of uncertainty in the form of fixed bias in the sensor data. In this paper, we extend the method to work with random errors in the sensor data, which is more realistic. Using a real building testbed, we show how performing an uncertainty analysis can reveal trends about inverse model accuracy and control performance, which can be used to make informed decisions about sensor requirements and data accuracy.

I. Introduction

Control-oriented models are needed to enable optimal control in buildings. Models for building load requirements, temperature dynamics and building systems are difficult to capture as each building is designed and used in a different way and therefore, it has to be uniquely modeled. Learning mathematical models of buildings from sensor data has a fundamental property that the model can only be as accurate and reliable as the data on which it was trained. Any sensor measurement exhibits some difference between the measured value and the true value and, therefore, has an associated uncertainty. Non-uniform measurement conditions, limited sensor calibration, the amount of sensor data and the amount of excitation of the plant make the measurements in the field vulnerable to errors. In the case of using sensor data for training inverse models (e.g., grey box or black box), the goal is to provide maximum benefit, in terms of model accuracy, for the least sensor cost. In this effort, we have developed a toolbox to investigate methods for low-cost building model capture by accounting for uncertainty propagation from sensors (type, density, placement) to model accuracy, and consequently, the operation cost of model-based control.

Small and medium sized buildings constitute more than 90% of the commercial buildings stock, but only about 10% of such buildings are equipped with a building automation system [1]. Current approaches for modeling buildings is cost-prohibitive for such buildings and they are unable to benefit from optimal supervisory control with model-based control schemes. An approach to obtaining the necessary data for generating building models involves installing temporary sensors and measuring the necessary model inputs and outputs to enable training and testing of the model. A report by the Department of Energy (DoE)[2] also emphasizes a program focused on adapting wireless sensors into an inexpensive retrofit system for energy-efficiency optimization of buildings.

The question of interest here is: *How do we determine the most important sensors and their best placement to minimize the cost of model capture and, consequently, reduced operation cost for building controls.* This provides a direct economic value by reducing the set of sensors needed as inputs for the control of the heating ventilation and air-condition system (HVAC). The quality of the model training data, characterized by uncertainty, depends on the accuracy of sensors, sensor placement and density. To evaluate the impact of uncertainty, we provide a method so the practitioner can clearly and easily assess the affect of input data quality on building modeling and control.

In [3], we presented a technique to quantify the effect of data uncertainty on building inverse model accuracy and control performance. However, that work only considers uncertainty in the form of fixed biases in sensor data. In this paper, we extend our method and toolbox to work with uncertainty in the form of random errors or random biases, which is more realistic.

This paper has the following contributions:

1) We present a toolbox for offline assessment of the influence of random bias in the input-output data on the accuracy of the inverse grey-box model.
2) We present a statistical method to quantify the bias of the sensor measurements due to their location and density, especially when it is measuring a spatially varying quantity, such as temperature. Our method can also be used for identifying near optimal sensor placement and density for a zone.
3) We evaluate both the uncertainty analysis and the sensor placement methods of the toolbox with case studies using data from real buildings.

A. Sources for Uncertainty in Building Modeling

Assessing the effect of uncertainties aids the understanding of building performance and, therefore, leads to effective

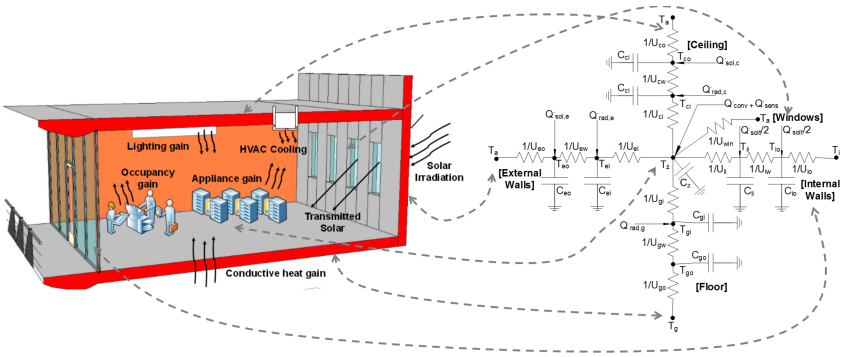

Fig. 1: RC lumped-parameter model representation for a thermal zone obtained from information about the zone geometry and usage.

decision making. The uncertainty in the model training data can be characterized in two ways: fixed error or random error. Fixed error can also be referred to as the systematic error, precision or fixed bias. The fixed error in the sensor measurement is due to a combination of two reasons. The first reason is the sensor precision. The best corrective action in this case is to ascertain the extent of the error (using the data-sheet or by re-calibration) and to correct the observations accordingly. The sensor may also exhibit a fixed error due to its placement, especially if it is measuring a physical quantity which has a spatial distribution, e.g., air temperature in a zone. In this case, it is hard to detect or estimate the bias unless additional spatially distributed measurements are obtained.

Measurement noise, sensor location and unknown extraneous conditions can cause the sensor reading to take some random values distributed about a mean. Errors (fixed or random) in the model training data adversely influence the accuracy of the building model which in turn affects the performance of the model based controller – which is the focus of this paper.

Organization: We begin with a short primer on the inverse modeling process for buildings in Section III. The input uncertainty analysis for inverse models within the IMPACT toolbox is presented in Section IV. Section V presents a case study in which we demonstrate our approach on sensor data obtained from a real building. Section VII concludes the paper with a discussion on the use of the free and open-source IMpACT toolbox.

II. Buildings Inverse Modeling

The main objective of an HVAC system for air temperature control is to reject disturbances due to outside weather conditions and internal heat gain caused by occupants, lighting and plug-in appliances. Therefore, the building model must accurately capture the thermal response of the building to the different disturbances. The building environment comprises of a complex set of interactions of heat, mass and momentum transfers. These transfers interact dynamically under the action of occupant and system control. The problem of representing such time varying interactions in a manner suitable for prediction and evaluation of alternate designs can be broadly classified into three model categories:

1) *White-box* models are based on the laws of physics and permit high fidelity modeling of the building system. Simulation programs like EnergyPlus and TRNSYS [4] fall into this category. Such models are unsuitable for control design due to their high level of complexity and large number of parameters. Furthermore, model capture and parameter tuning is time consuming and not cost effective.
2) *Black-box models* are not based on physical behaviors of the system but rely on the available data to identify the model structure (e.g., regression methods and neural-nets) These models are often purely statistical provide little insight into the dynamics dictating the system behavior.
3) *Grey-box models* fall in between the two above categories. A simplified model structure is chosen loosely based on the physics of the system and the available data is used to estimate the values of the model parameters. These models are suitable for control design and still respect the physics of the system.

A. Model Structure

A commonly used grey-box representation of the thermal response of a building due to heat disturbances uses a lumped parameter Resistive-Capacitative (RC) network. The building fabric is described in terms of orientation, area, material thickness, density, conductivity, specific heat capacity, surface shortwave absorptivity and long-wave emissivity to enable calculation of heat transfers. This approach has been used widely, e.g., in [5], [6], [7].

Figure 1 shows an example of such a model for a single zone, as used in [5]. In this representation, the central node of the RC network represents the zone temperature $T_z(^\circ\text{C})$. The geometry of the zone is divided into different kinds of surfaces, each of which is modeled using a 'lumped-parameter' branch of the network. The zone is subject to several (heat) disturbances which are applied at different nodes in the network in the following manner: (a) solar irradiation on the external wall $\dot{Q}_{sol,e}(\text{W})$ and the ceiling $\dot{Q}_{sol,c}(\text{W})$ is applied on the exterior node, (b) incident solar radiation transmitted through the windows $\dot{Q}_{solt}(\text{W})$ is assumed to be absorbed by the internal and adjacent walls, (c) radiative internal heat gain $\dot{Q}_{rad}(\text{W})$ is distributed with an even flux to the walls and the ceiling, (d) the convective internal heat gain $\dot{Q}_{conv}(\text{W})$ and the sensible cooling rate $\dot{Q}_{sens}(\text{W})$ is applied directly to the zone air, (e) the zone is also subject to heat gains due to the ambient temperature $T_a(^\circ\text{C})$, ground temperature $T_g(^\circ\text{C})$ and temperatures in other zones which are accounted for by adding boundary

condition nodes to each branch of the network. The list of all parameters in the model is given in Table I. The nodal equations for the external wall network are:

$$\begin{aligned} C_{eo}\dot{T}_{eo}(t) &= U_{eo}(T_a(t) - T_{eo}(t)) + U_{ew}(T_{ei}(t) - T_{eo}(t)) + \dot{Q}_{sol,e}(t) \\ C_{ei}\dot{T}_{ei}(t) &= U_{ew}(T_{eo}(t) - T_{ei}(t)) + U_{ei}(T_z(t) - T_{ei}(t)) + \dot{Q}_{rad,e}(t) \end{aligned} \tag{1}$$

Similarly, one can write the equations for the dynamics of the nodes of the floor, the ceiling and internal wall network. The law of conservation of energy gives us the following heat balance equation for zone

$$\begin{aligned} C_z\dot{T}_z(t) = {} & U_{ei}(T_{ei}(t) - T_z(t)) + U_{ci}(T_{ci}(t) - T_z(t)) \\ & + U_{ii}(T_{ii}(t) - T_z(t)) + U_{gi}(T_{gi}(t) - T_z(t)) \\ & + U_{win}(T_a(t) - T_z(t)) + \dot{Q}_{conv}(t) + \dot{Q}_{sens}(t) \end{aligned} \tag{2}$$

Differential equations (1) and (2) are combined to give a state space model of the system. Define $x = [T_{eo}, T_{ei}, T_{co}, T_{ci}, T_{go}, T_{gi}, T_{io}, T_{ii}, T_z]^T$ as the state vector of all temperatures. The input u is a vector of all the inputs to the systems, i.e., $u = [T_a, T_g, T_i, \dot{Q}_{sol,e}, \dot{Q}_{sol,c}, \dot{Q}_{rad,e}, \dot{Q}_{rad,c}, \dot{Q}_{rad,g}, \dot{Q}_{solt}, \dot{Q}_{conv}, \dot{Q}_{sens}]^T$. The elements of the system matrices depend non-linearly on the parameters U and C. Consider $\theta = [U_{eo}, U_{ew}, U_{ei}, \ldots C_{io}, C_{ii}]^T$ as a vector of all the model parameters. The state space equations have the following representation emphasizing the parameterization of the system matrices.

$$\begin{aligned} \dot{x}(t) &= A_\theta x(t) + B_\theta u(t) \\ y(t) &= C_\theta x(t) + D_\theta u(t) \end{aligned} \tag{3}$$

This model is based on the assumption that the air inside the zone is well mixed and hence it can be represented by a single node. Only one-dimensional heat transfer is assumed for the surfaces. The parameters of the model are assumed to be time invariant.

B. Parameter Estimation (Model Training)

The goal of parameter estimation is to obtain estimates of the parameter vector θ from input-output time series measurement data. The parameter search space is constrained both above and below by $\theta_l \leq \theta \leq \theta_u$. For a given parameter vector θ, the model, given by (3), can be used to generate a time series of the zone air temperature T_{z_θ} using the measured time series data for the inputs $u(k)$. The subscript θ denotes that the temperature value T_{z_θ} is the predicted value using the model with parameters θ and the inputs u. This model generated time series T_{z_θ} is compared with the observed values of the zone temperature T_{z_m}, and the difference between the two is quantified by a statistical metric. The metric chosen is the sum of the squares of the differences between the two time series. The parameter estimation problem is to find the parameters θ^*, subject to $\theta_l \leq \theta \leq \theta_u$, which lead to the least square error between the predicted and the measured temperatures, i.e.,

$$\theta^* = \underset{\theta_l \leq \theta \leq \theta_u}{\arg\min} \sum_{k=1}^{N} (T_{z_m}(k) - T_{z_\theta}(k))^2 \tag{4}$$

where the summation is over the N data points of the input-output time series under investigation.

The least square optimization of (4) is a constrained minimization of a non-linear objective. It is numerically solved using a trust region reflective algorithm such as the Levenberg-Marquardt [8] algorithm. The parameters of grey-box models usually have physical meanings, it is desirable that the initial parameter estimates θ_0 are as close as practicable to their (unknown) optimal (true) values. The initial values of the parameters can be estimated from the building structure and materials.

TABLE I: List of parameters

$U_{\star o}$	convection coefficient between the wall and outside air
$U_{\star w}$	conduction coefficient of the wall
$U_{\star i}$	convection coefficient between the wall and zone air
U_{win}	conduction coefficient of the window
$C_{\star\star}$	thermal capacitance of the wall
C_z	thermal capacity of zone z_i
	g: floor; e: external wall; c: ceiling; i: internal wall

III. IMPACT: UNCERTAINTY PROPAGATION ANALYSIS

We now describe the approach for analyzing uncertainty propagation for building inverse models. Methods within this approach require multiple simulations of systematically altered models and the subsequent analysis of the differences in the appropriate output in order to draw conclusions on the effect of uncertainty. The accuracy of the building inverse model depends primarily on the following three factors:

(a) **The structure of the model** which depends on the extent to which the model respects the physics of the underlying physical system,
(b) **The performance of the estimation algorithm**. The performance of of non-linear estimation depends heavily on the nominal values of the parameters.
(c) **The quality of the training data**, which can be characterized by its uncertainty.

The main premise of the input uncertainty propagation is that once the model structure and the parameter algorithm are fixed, one can study the influence of the uncertainty in the training data on the accuracy of the model using simulations which utilize artificial data sets. We introduce a random bias in each of the training data streams in form of perturbations around the nominal values. This results in the creation of artificial training data sets, each of which is similar to the original unperturbed data set except for one input data stream. For each artificial data set, we train a new inverse model and calculate its test error. A common test data-set is used to compare the accuracy of the models in terms of their test root mean square error (RMSE). This quantifies the effect of uncertainty in each input on the accuracy of the inverse model.

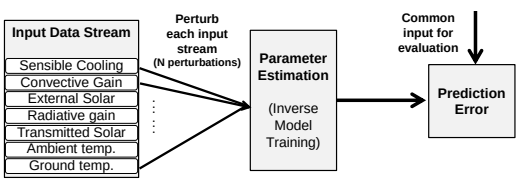

Fig. 2: Overview of the IMpACT input uncertainty analysis methodology, an offline method to confirm the influence of each training input on the accuracy of the model.

A. Input Uncertainty Analysis

The aim of this analysis is to determine the influence of bias in the training data inputs on the accuracy of the inverse model and then, to quantify the relative importance of the inputs. First, some notation is introduced for brevity. We consider a model with $m > 0$ training input data sets denoted by $V = \{v_1, \cdots, v_m\}$. Note that these are inputs for model training, not the inputs for the model itself, e.g., even though zone temperature is a model output, it is still a required data-set (hence, an input) for model training. $V_{i,\delta} = \left\{\hat{v_i} = v_i + \delta, v_j = v_j | i, j \leq m, j \neq i, \delta = \mathcal{N}(\mu_i, \sigma^2)\right\}$ denotes the artificial data-set obtained by perturbing input v_i by an random Gaussian perturbation $\delta \sim \mathcal{N}(\mu_i, \sigma^2)$ with mean μ_i and variance σ^2 while keeping all other input data-sets unperturbed. V_0 denotes the data-set in which all the inputs are unperturbed. Now, $\hat{M}_{V_{i,\delta}}$ is the inverse model with obtained by training on the data-set $V_{i,\delta}$ and $\hat{M}_{V_0}$ is the model obtained by training on a completely unperturbed data-set. The approach for conducting an input uncertainty analysis consists of the following steps:

(a) Establish a baseline (reference) model: The baseline model, $\hat{M}_{V_0}$, is the inverse model obtained by training on the unperturbed data set V_0, which is considered as the ground truth.
(b) Determine which model outputs will be investigated for their accuracy and what are their practical implications.
(c) Each of the input data streams are then perturbed within some bounds. There are a total of N perturbations $\delta_1, \cdots, \delta_N$ ($\delta_i \sim \mathcal{N}(\mu_i, \sigma^2)$) for each input stream $u_i, i \leq m$. For each perturbation δ_i, the mean μ_i of the Gaussian error is changed while keeping the variance the same. This results in N artificial data-sets $V_{i,\delta_1}, \cdots, V_{i,\delta_N}$ for each input stream i.
(d) Corresponding to every perturbation, the inverse modeling process is run again and a new model $\hat{M}_{V_{i,\delta_k}}$ is obtained.
(e) The prediction accuracy of each of the trained model is evaluated on a common input data stream V_T. The accuracy of the model $\hat{M}_{V_{i,\delta_k}}$ is measured by the RMSE $r(\hat{M}_{V_{i,\delta_k}})$ between the predicted and the actual model output values for the common input stream V_T.
(f) Using the RMSE of the fit and the magnitude of the perturbation, the sensitivity coefficient for each input training stream is determined. It is calculated as follows:

$$\gamma_i = \underset{k=1,\cdots,N}{\text{mean}} \left(\frac{r(\hat{M}_{V_{i,\delta_k}}) - r(M_{V_0}) / r(M_{V_0})}{|\delta_k|} \right) \quad (5)$$

where, $|\delta_k|$ is the mean of the k^{th} random perturbation. The input uncertainty analysis method is shown in Figure 2.

The magnitude of the sensitivity coefficient γ_i can be interpreted as the mean value of the change in the RMSE of the model due to the presence of a random error in the input data-set. It is the mean of the ratio of the normalized change in the model accuracy to that of the normalized magnitude of the perturbation in the input data. The sensitivity coefficient is also referred to as the influence coefficient or point elasticity. The sensitivity coefficients are calculated for each training input data-set and then compared to reveal the significance of the inputs in terms of their influence on the inverse model accuracy.

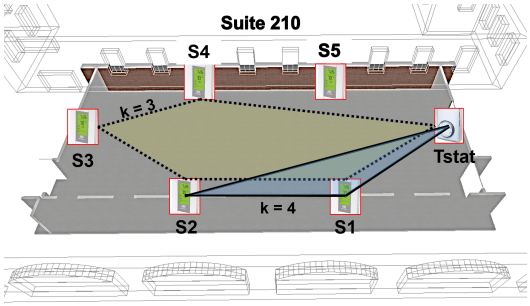

Fig. 3: Temperature sensor locations for suite 210. The thermostat (Tstat) is located on the south (right) wall.

Although the method presented here assumes a specific model structure (i.e., state-space), the IMpACT toolbox's input uncertainty analysis approach is general and will work for any building inverse model (i.e., any model structure and the accompanying estimation algorithm).

IV. Case Study with Real Data

In this section we present the results of applying the input uncertainty analysis to real sensor data. The site chosen for analysis is called Building 101. Located in Philadelphia, it is the headquarters of the U.S. DoE's Energy Efficient Building Hub [9]. It is a highly instrumented commercial building where the acquired data is made available to researchers. We focus on suite 210, a large office space on the second floor of the north-wing of the building. This zone has a single external wall on the east side with 8 windows, a large interior wall on the west side which is adjacent to the porch area on the north-wing and two more adjacent walls on the north and the south side. On July 20, 2013, functional tests were run from 00:00 to 22:29, on the air handling unit serving suite 210. During a functional test, the supply air temperature is changed rapidly so there is enough thermal excitation in the zone to generate a rich data-set for learning its dynamical model.

A. Sensor Placement and Data Quality

We first show how the location of a sensor can affect the quality of measured data and also present a statistical method to determine the optimal sensor placement and density for obtaining high quality data. Our aim was to analyze the temperature data from suite 210 to determine if there is any significant location bias in the thermostat reading and to study how adding additional temporary sensors to a location changes the accuracy of the data. It should be pointed out that the thermostat reading is the one which is used for controlling the zone temperature so any biases/errors in the temperature measurement are not desired. There are a total of six different locations (S_1,S_2,S_3,S_4,S_5 and $Tstat$) in suite 210 where air temperature is logged, as shown in Figure 3. The zone thermostat ($Tstat$) is placed on the south wall.

The true value of the temperature of a zone (air volume) is extremely hard to determine. Since the different temperature sensors are located around the zone in a uniform manner, the mean of all six temperature measurements is a better

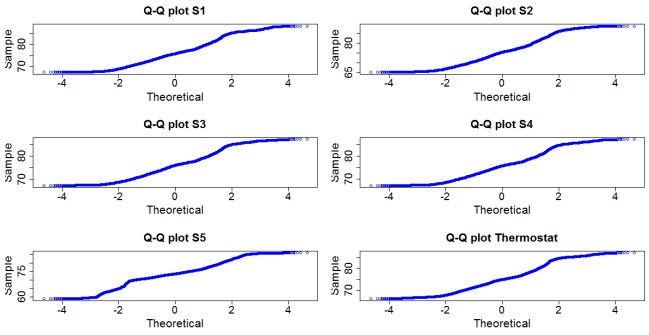

Fig. 4: Q-Q plot for the temperature data from all the locations show that the temperature data is not likely to be normally distributed.

representation of the zone temperature and is regarded as the *true* temperature (denoted by T_{tr}). We wanted to estimate the bias due to sensor location and to determine the best sensor placement and density. For this, we select k sensors ($k = 1, 2, \cdots, 5$) out of the six available sensors and compare the average temperature T_k of the selected k sensors with the *true* temperature T_{tr} through hypothesis testing.

We first check the normality of the temperature data from each sensor using a quantile-quantile (Q-Q) plot. The Q-Q plot is used to check the validity of a distributional assumption for a data-set. The idea is to compute the theoretically expected value for each sample based on the distribution in question. If the temperature data follow a normal distribution, then the points on the normal Q-Q plot will fall on a straight line. Figure 4 shows the Q-Q plot for the data from all six sensors against the theoretical samples obtained from normal distribution. The plots suggest that the temperature data is not normally distributed and is likely to follow a distribution with thicker tails than the normal distribution. This implies that the t-test is no longer the best test for comparing any two data-sets as it assumes that the data is normally distributed.

To overcome this problem, we use non-parametric statistics for comparing temperature data-sets against each other. In particular, we use the Wilcoxon rank-sum statistic. The Wilcoxon test is valid for data from any distribution, whether normal or not, and is much less sensitive to outliers than the t-test. It is suitable for testing differences between paired data-sets, for e.g., comparing the air temperature measurements from two different sensors sampling at the same rate. While comparing any data-set T_k to the *true* temperature T_{tr} we check the hypothesis that the two data-sets are originating from the same distribution and that the median difference between pairs of observations is zero. The Wilcoxon's test provides an estimate μ_k (*Hodges-Lehmann estimate*) and the 95% confidence interval (C.I.) of the bias between the two data-sets.

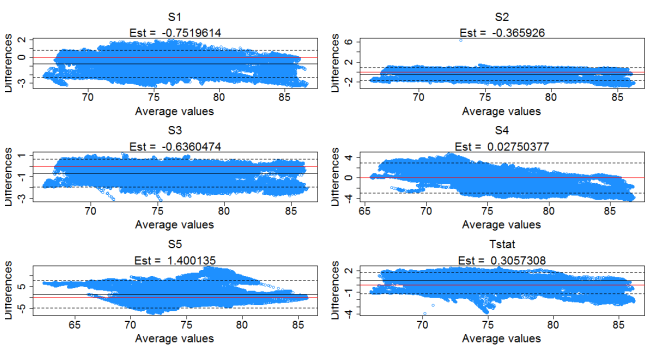

Fig. 5: Bland-Altman plots for all 6 sensors i.e., $k = 1$. The solid red line indicates the mean difference between the *true* temperature and the data-set. The estimated bias is obtained through the Wilcoxon's test.

An intuitive, but informal, method of comparing the *true* temperature with another data-set by visual inspection is through the Bland-Altman plot also known as Tukey's mean difference plot. In this method, the difference of the two paired data-sets is plotted against their mean. Figure 5 shows Bland-Altman plots for the case $k = 1$, i.e., each sensor measurement (T_{S_1},T_{S_2},T_{S_3},T_{S_4},T_{S_5} and $Tstat$) is compared with the *true* temperature T_{tr}. The estimate of the bias μ_k between the data-sets and the *true* temperature obtained through the Wilcoxon's test is also indicated for each data-set. For the case $k = 1$, there are 6 possible comparisons with the *true* temperature. It turns out that the sensor location S_4 is the closest to the *true* temperature with an estimated bias of only 0.027°C. The thermostat measurement $Tstat$ has an estimated bias of 0.588°C with respect to the *true* temperature. This means that if we were to place just one sensor in the zone to estimate the *true* temperature, it should be placed at the location of $S4$. The next section evaluates whether the bias in the zone thermostat is enough to affect the model accuracy.

The same method is repeated for each value of $k = (1, 2, \cdots, 5)$. For each k, all $\binom{6}{k}$ sensor combinations are enumerated and the mean temperature T_k of the k selected sensors is compared with the *true* temperature using the same techniques as described above. The combination with the minimum bias estimate μ_k is selected as the best sensor subset for each value of k. The results of these comparisons are summarized in Table II.

The results indicate that adding multiple sensors to a zone tends to improve the accuracy of the quantity being measured. However, it is not always the case that adding additional sensor will always lead to an improvement in data accuracy. This can be seen from Table II where the bias in the combined measurement of the data obtained from 3 sensors is much less than the bias due to the combined measurement obtained from 4 different sensors. The minimum bias sensor subset for $k = 3$ and $k = 4$ is also shown in Figure 3.

B. Input Uncertainty Analysis for Suite 210

We created the lumped parameter RC-network model for suite 210 using the principles described in Section III. The model has 9 states, 9 inputs and 1 output. There are a total of 22 RC parameters in the model structure for this zone.

TABLE II: Wilcoxon's test results for all values of k

k	Min. bias subset T_k	Bias Estimate μ_k
1	S_4	0.0275
2	S_3, S_4	-0.0106
3	S_1, S_2, $Tstat$	0.00708
4	S_1,S_3,S_4, $Tstat$	0.22
5	S_1,S_3,S_4,S_2,$Tstat$	-

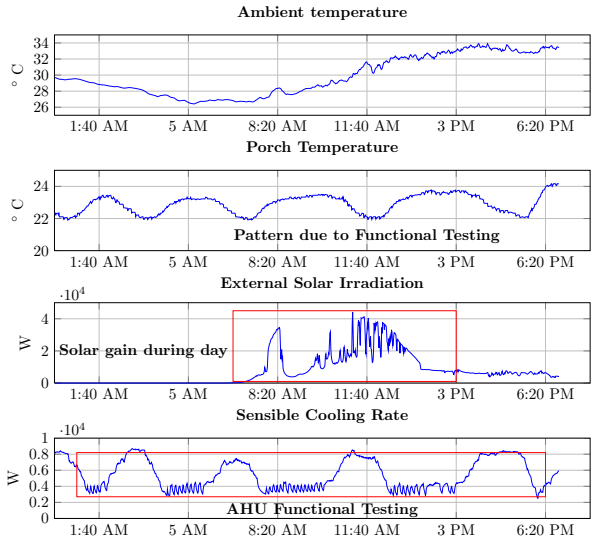

Fig. 6: Training data for suite 210 of Building 101. The data obtained by running a functional test on the zone's air handling unit from 20-07-2013 00:00 to 20-07-2013 22:29

This model can be used for advanced control methods such as model predictive control (MPC).

The temperature inputs to the model were the ambient temperature $T_a(°\text{C})$, floor temperature $T_f(°\text{C})$, ceiling temperature $T_c(°\text{C})$ and temperature of the adjacent porch area $T_p(°\text{C})$. The external solar irradiation Q_{sole} is logged by a pyranometer. For the internal heat gain calculation, we consider 3 different heat sources: occupants, lighting and appliances. The number of people in the zone at different times was estimated using data from people counters. We assume, using ISO standard 7730, that in a typical office environment the occupants are seated, involved in light activity and emit 75 (W) of total heat gain, 30% of which is convective and 70% is radiative gain. Using the power rating of the lighting fixtures and their efficiency, one can calculate the heat gain due to lighting. In this zone, lights contribute about 13 (W/m^2) with a $40\% - 60\%$ split between the convective and the radiative part. A constant heat gain due to the electrical appliances and computers is also assumed. The total internal convective heat gain Q_{conv} was obtained by adding the convective gain contributions from the three different heat gain sources. The total internal radiative heat gain was obtained in a similar way. The total internal radiative gain is further split into the radiative gain on the external wall Q_{qgrade} and on the ceiling Q_{qgradc}. The sensible cooling rate Q_{sen} was calculated using the temperature and mass flow rate measurements for the supply and the return air.

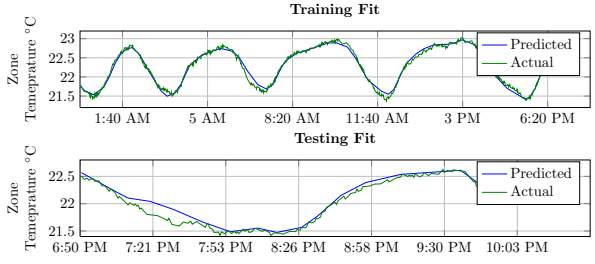

Fig. 7: Fit between the predicted and actual zone temperature in suite 210. Top: for the training period, with RMSE = 0.062 and $R^2 = 0.983$. Bottom: for the test period with RMSE = 0.091 and $R^2 = 0.948$.

The total available data was split into a training set (80%) and a test set (20%). Some of the inputs for training the inverse model are shown in Figure 6. The output of the model is the zone temperature T_z. The results of the inverse model training are shown in Figure 7. The RMSE for the training data-set was $0.062(°\text{C})$ with R^2 equal to 0.983 (Figure 7, top) while the RMSE and R^2 values for the test set were $0.091(°\text{C})$ and 0.948 respectively (Figure 7, bottom).

After successfully training the inverse model, we conducted an input uncertainty analysis on the training data-set as described in Section IV-A. The model trained on unperturbed data serves as the baseline model for the uncertainty analysis. We created artificial data-sets from the training data by perturbing each training input, one at a time, by adding a random bias to the nominal data-set. The random bias in the temperature measurements was varied between $[-3, 3]°\text{C}$ in increments of $0.2°\text{C}$ and the variance was held constant at 1. For the heat gains and the sensible cooling load the mean of the Gaussian random perturbation was varied between $[-300, 300]\text{W}$. The range for the perturbation was calculated based on the estimated uncertainty due to the characteristics of the physical sensor and due to the method of inference of the data (for internal heat gains).

With 30 additional data-sets per input, there were a total of 300 artificial data-sets. Each of these data-sets were used for model training and the resulting model was evaluated for its accuracy (RMSE) on the test-set.

C. Results

The results of the input uncertainty analysis for suite 210 in Building 101 are shown in Figure 8. We see a parabolic trend obtained as a result of "artificial" uncertainty in the training data for each of the training data-sets. This aligns well with the intuition that as the magnitude of the uncertainty bias increases in the input data stream, the inverse model becomes worse and its prediction error increases. This is the case for all the input data streams and it results in the parabolic trend. The shape of the curve varies from input to input, due to a different sensitivity coefficient value, and is an indicator of the extend to which a particular input influences the model accuracy. The sensitivity coefficients for the different training inputs were calculated. Figure 9 shows the comparison of the model accuracy sensitivity coefficients for the inverse model for suite 210.

It is seen that the zone temperature has the largest model accuracy sensitivity coefficient suggesting that the accuracy of the model is quite sensitive to the zone temperature measurement. We saw in Section V-A that the thermostat measurement has an uncertainty bias of about $0.588°\text{C}$. From figure 8(j), we see that this can effect the model accuracy on by up to 13%. This suggests that for this zone, it would be better to deploy additional low-cost wireless sensors just during the model training phase and get a better estimate of the zone temperature for training the inverse model. Also, the mean value obtained by adding more sensors could be used to re-calibrate or correct the thermostat reading for location bias, resulting in data which can yield an inverse model which can better represent the dynamics of the zone.

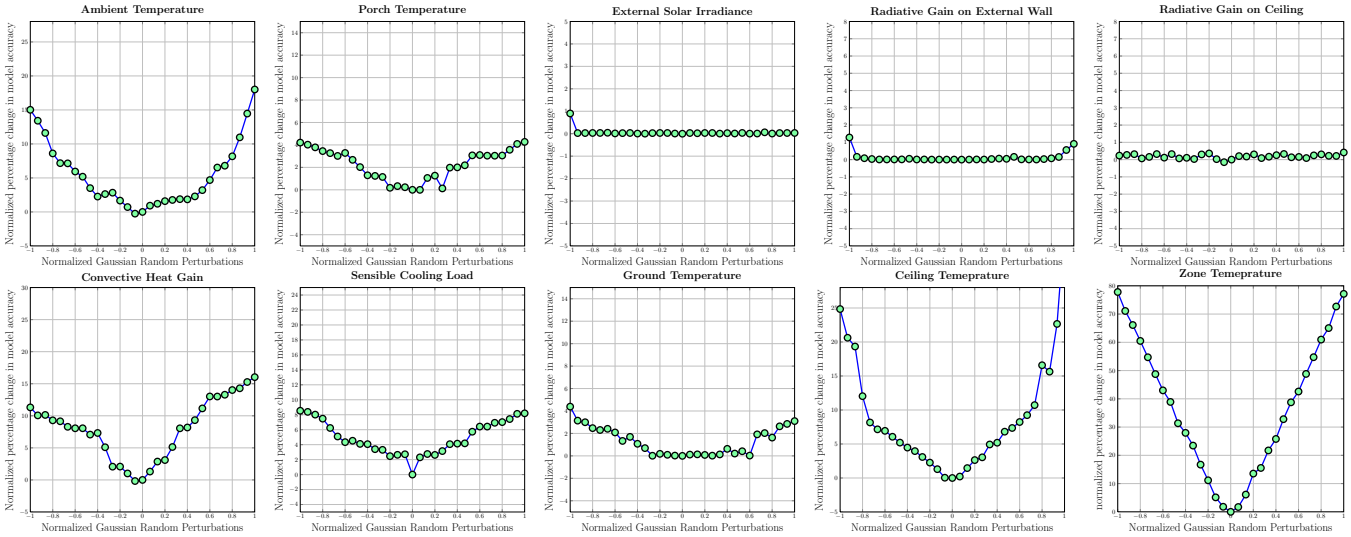

Fig. 8: The x axis shows the normalized Gaussian perturbation introduced in the data while the y axis is the normalized change in the model accuracy (RMSE). The following inputs are shown: (a) ambient temperature (°C); (b) porch temperature (°C); (c) incident solar irradiation on the external walls (W); (d) and (e) radiative internal heat gain on external wall and ceiling (W); (f) convective internal heat gain (W); (g) sensible cooling rate (W); (h) floor temperature (°C); (i) ceiling temperature (°C), and (j) zone temperature (°C)

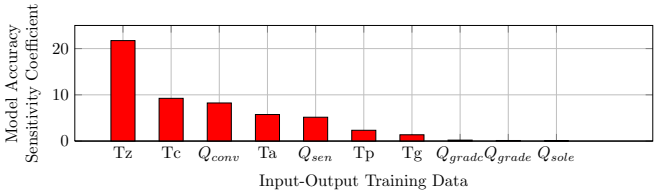

Fig. 9: Model accuracy sensitivity coefficients for Building 101

Although the IMpACT approach has been presented for the case of a single zone, it can be easily extended for a multi-zone scenario in which zones interact with each other.

Model Accuracy and Control Performance: The IMpACT toolbox has been presented as a means of conducting an automated input uncertainty analysis. However, the toolbox also has the capability to relate model accuracy to control performance for a complete end-to-end treatment of uncertainty propagation. This is based on our previous work [3], in which we present the method for establishing the relationship between model accuracy and the performance of a model predictive controller. We showed (Figure **??**) that the potential savings of MPC deteriorate rapidly as the model accuracy decreases (i.e., test RMSE increases). By empirically establishing a relationship between model accuracy and MPC performance, one can take informed decisions about the investment on additional sensors and the associated cost benefit for improving the data quality.

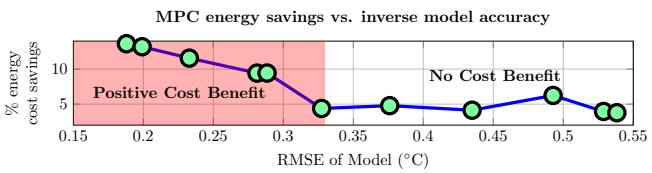

Fig. 10: MPC performance for models of different degrees of accuracy. In the left region there is a positive cost benefit associated with adding sensors but in the right region there is no cost benefit associated with adding additional sensors.

V. Related Work

Parametric sensitivity analysis of a model reveals the important parameters of the model which most significantly affect the model output. This bears some resemblance with the way the input uncertainty analysis is conducted in the IMpACT toolbox. In [10], important design parameters are identified from points of view of annual building energy consumption and peak loads. In [11], the authors extend traditional sensitivity analysis and increase the size of analysis by studying the influence of about 1000 model parameters.

It is only recently in [12], [13] and [14], that researchers have analyzed the uncertainty propagation in modeling for close loop control. In [12], the authors acknowledge that the performance of advanced control algorithms depends on the estimation accuracy of the parameters of the model. In [13], the authors discuss the development of a control-oriented simplified modeling strategy for MPC in buildings using virtual simulations. [14] presents a methodology to automate building model calibration and uncertainty quantification using large scale parallel simulation runs. In [15], the authors consider the co-design of the sensing and the control platform for buildings. They also present a case study with mutli-point temperature measurements of the same space to quantify the effect of sensor location on the measurement. However, they do assume that the measurement error has a Gaussian distribution, whereas our analysis is non-parametric and distribution free. In recent work [16], researchers have utilized computation fluid dynamic models to figure out the best sensor placement for state estimation for optimal control.

VI. Conclusion

We introduced IMpACT, a methodology and a toolbox for analysis of uncertainty propagation for building inverse modeling and controls. Given a plant model and real input data, IMpACT automatically evaluates the effect of the uncertainty propagation from sensor data to model accuracy and control

performance. The extent of the influence of uncertainty in each training data stream on the model accuracy can be quantified through an input uncertainty analysis. We run the IMpACT toolbox on a data-set obtained from a real building and show that the density and placement of sensors are responsible for introducing a location based bias in the measured data. We observe that a bias of $\sim 0.6°\text{C}$ in the zone temperature degrades the model accuracy by $\sim 13\%$ for the zone. We also presented a statistical method to quantify the bias in the sensor measurement (if any) and to determine near optimal sensor placement and density for accurate data measurements. One limitation of the input uncertainty analysis is that it assumes independence between training inputs and analyzes them one by one. It may be the case that the model training inputs are not independent. This will require better sampling methods (factorial sampling, latin hypercube sampling) for perturbing multiple inputs at the same time. We are continuing our efforts to develop IMpACT into a an open source toolbox to automate the input uncertainty analysis for building inverse models.

REFERENCES

[1] S. Katipamula *et al.*, "Small-and Medium-Sized Commercial Building Monitoring and Controls Needs: A Scoping Study," Pacific Northwest National Laboratory (PNNL), Richland, WA (US), Tech. Rep., 2012.

[2] R. Butters, A. Schroeder, G. Hernandez, P. Fuhr, T. McIntyre, and W. Manges, "US Department of Energy Advanced Sensing and Controls for Energy Efficient Buildings: A Cross Cutting Project," in *ACEEE Summer Study on Energy Efficiency in Industry*, 2011.

[3] M. Behl, T. Nghiem, and R. Mangharam, "Model-iq: Uncertainty propagation from sensing to modeling and control in buildings," *ACM/IEEE International Conference on Cyber-Physical Systems*, 2014.

[4] D. B. Crawley, J. W. Hand, M. Kummert, and B. T. Griffith, "Contrasting the Capabilities of Building Energy Performance Simulation Programs," *Building & Environment*, vol. 43, no. 4, pp. 661–673, 2008.

[5] J. E. Braun and N. Chaturvedi, "An inverse gray-box model for transient building load prediction," *HVAC and R Research*, vol. 8, no. 1, pp. 73–99, 2002.

[6] T. L. McKinley and A. G. Alleyne, "Identification of Building Model Parameters and Loads using On-site Data Logs," *Third National Conference of IBPSA-USA*, 2008.

[7] T. Dewson, B. Day, and A. Irving, "Least Squares Parameter Estimation of a Reduced Order Thermal Model of an Experimental Building," *Building and Environment*, vol. 28, no. 2, pp. 127–137, 1993.

[8] J. J. Moré, "The levenberg-marquardt algorithm: implementation and theory," *Numerical analysis*, pp. 105–116, 1978.

[9] US Department of Energy. (2013, Oct.) EEB Hub: Energy efficient buildings hub. [Online]. Available: http://www.eebhub.org/

[10] J. C. Lam and S. Hui, "Sensitivity analysis of energy performance of office buildings," *Building & Environment*, vol. 31, pp. 27–39, 1996.

[11] B. Eisenhower, Z. O'Neill, V. A. Fonoberov, and I. Mezić, "Uncertainty and sensitivity decomposition of building energy models," *J. Building Perf. Simulation*, vol. 5, pp. 171–184, 2012.

[12] S. Bengea, V. Adetola, K. Kang, M. J. Liba, D. Vrabie, R. Bitmead, and S. Narayanan, "Parameter estimation of a building system model and impact of estimation error on closed-loop performance," in *Decision and Control and European Control Conference (CDC-ECC), 2011 50th IEEE Conference on*, 2011, pp. 5137–5143.

[13] J. A. Candanedo, V. R. Dehkordi, and P. Lopez, "A control-oriented simplified building modelling strategy," in *13th Conf. Intl. Building Perf. Simulation Ass.*, 2013.

[14] S. N. Slaven Peles, Sunil Ahuja, "Uncertainty quantification in energy efficient building performance simualtions," in *International High Performance Buildings Conference*, 2012.

[15] M. Maasoumy, Q. Zhu, C. Li, F. Meggers, and A. Vincentelli, "Co-design of control algorithm and embedded platform for building hvac systems," in *Cyber-Physical Systems (ICCPS), 2013 ACM/IEEE International Conference on*, April 2013.

[16] J. A. Burns, J. Borggaard, E. Cliff, and L. Zietsman, "An optimal control approach to sensor/actuator placement for optimal control of high performance buildings," 2012.